Chinese Chemical Letters 35 (2024) 108534

Contents lists available at ScienceDirect

Chinese Chemical Letters

journal homepage: www.elsevier.com/locate/cclet

Highly efficient labelling of extracellular vesicles for enhanced detection on a microfluidic platform

Shi Hu[1], Rui Hao[1], Zitong Yu, Huitao Zhang, Hui Yang*

Bionic Sensing and Intelligence Center, Institute of Biomedical and Health Engineering, Shenzhen Institute of Advanced Technology, Chinese Academy of Sciences, Shenzhen 518055, China

ARTICLE INFO

Article history:
Received 2 December 2022
Revised 7 April 2023
Accepted 2 May 2023
Available online 4 May 2023

Keywords:
Microfluidic platform
Extracellular vesicles
Labelling
PKH dye
Flow cytometry

ABSTRACT

Developing precise extracellular vesicles (EVs) labelling techniques with minimal disturbance is of great importance to the follow-up EVs detection and analysis. However, currently available methods such as using probes to conjugate phospholipids or membrane proteins have certain limitations due to EV steric hindrance, dye aggregation, *etc.* Here, we present a microfluidic platform to enhance EVs' labelling efficiency and improve their detection. This platform provides excellent sample throughput and high-efficiency EV labelling at lower label concentrations with an optimized flowing rate. Flow cytometry analysis (FCM) and cellular uptake results show that EV labelling by utilizing this platform possesses the merits of a higher labelling efficiency with 64.1% relative improvement than conventional co-incubation method and a lower background noise. Moreover, this technique maintains EVs' size, morphology and biological activities. After the recipient cells uptake the EVs treated by the microfluidic platform, the spatial and temporal distribution of EVs in the cells are clearly observed. These results demonstrate that our method holds great potential in efficient labelling of EVs, which is essential to subsequent EV quantification and analysis.

Extracellular vesicles (EVs) are a type of membranous vesicles secreted from cells to extracellular environment and then taken up by recipient cells, they participate in various pathophysiological processes and exist in cell culture mediums and biological fluids [1,2]. With the advantages of high concentration, less invasive sampling and carrying a variety of molecules that reflect the characteristics of parental cells, EVs play an important role in clinical diagnosis as novel liquid biopsy biomarkers [3,4]. However, sensitive detection and accurate visualization of EVs in large-scale research applications are severely limited due to their submicron size [5–7].

For precise and highly efficient detection of EVs, fluorescent labelling brings the advantages of high sensitivity and specificity, making it suitable for analysing these nanoscale biological particles [8]. Coventional EV fluorescent labelling approaches can be categorized as using either lipophilic dyes or fluorescent probes conjugated to membrane proteins [9–11]. However, the labelling by using fluorescent protein probes is hindered by their intrinsically large size and the low abundance of membrane proteins on EVs (CD9, CD63, CD81, *etc.*) [12,13]. As the most commonly used labelling probes, lipophilic dyes, including PKH26, PKH67, Dil, Dio and *etc.*, have the advantages of simple operation [12,14], high fluorescent intensity and small molecule size [15,16]. However, it is worth noting that during EV labelling procedures, lipophilic dyes aggregate at the concentration recommended by the manufacturer's instructions, generating false positive particles as the same size of EVs, resulting in "what you see is not what you get" [17,18]. Therefore, there is an urgent demand for techniques enabling EV labelling by using a minimal amount of dye that can reduce dye aggregation disturbance without sabotaging the labelling efficiency for precise quantification and analysis of EVs.

To solve the intrinsic conflict of using minimal amount of fluorescent dyes and achieving high EV labelling efficiency, it is necessary to find a method that can increase the contact opportunity between fluorescent dyes and EVs, and can accurately process nanoscale EVs. Microfluidic technology has attracted tremendous attention in bioanalytical applications due to its advantages such as fast response, low sample consumption, and good process control [19–21]. In recent years, this technology has shown great potential for rapid and efficient chemical reactions, as it decreases molecular diffusion length and accelerates the reaction between different molecules [22–25]. It was also reported that minimalis-

* Corresponding author.
E-mail address: hui.yang@siat.ac.cn (H. Yang).
[1] These authors contributed equally to this work.

https://doi.org/10.1016/j.cclet.2023.108534
1001-8417/

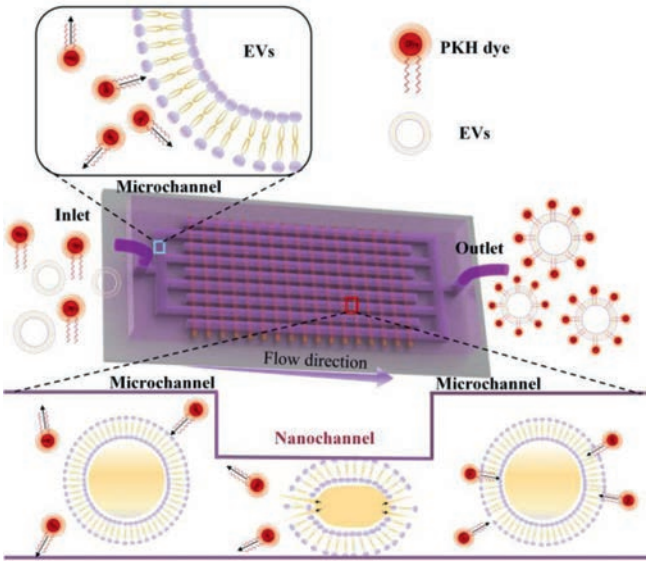

Fig. 1. Schematic illustration on the microfluidic platform for highly efficient EV labelling.

tic probes delivered to mammalian cells by microfluidic platform could achieve high-affinity and target-specific tracing of proteins in various subcellular compartments [26].

In this work, we investigate highly efficient EV labelling and quantification by utilization of a microfluidic platform to minimize fluorescent dye consumption, avoiding generating false positive signals (Fig. 1). We propose that at extremely low lipophilic dye concentrations, our microfluidic labelling platform can improve EV labelling efficiency and reduce dye aggregation by increasing the probability of dye contacting the EV membrane. Commercial lipophilic dyes are used to incorporate into the EV membrane. A flow cytometer (CytoFLEX S, Beckman Coulter, USA) is utilized to optimize the geometric design of the microfluidic platform and to evaluate its performance on EV labelling. Cellular uptake is conducted to observe the distribution of fluorescent EVs in cells. The biological activities of EVs treated by the microfluidic platform are verified by CCK-8 and cell wound scratch assay.

The microfluidic platform consists of a microchannel network and a nanochannel array, where the microchannels intersect the nanochannels (Figs. 2a and b). There are 10 microchannels linked to the platform inlet and 11 to the outlet, 1500 nanochannels are utilized to connect the inlet channels and the outlet ones, therefore, generating an interdigitated array with 30,000 nanochannels to process EVs. The width and height of the microchannels are much bigger than those of the nanochannels for sample transportation without generating much flow resistance. The width of each nanochannel is set to 2 μm, and the depth of the nanochannel is 130 nm that is comparable to the dimension of the EVs (Fig. 2c). Further details on the preparation of nanochannels are presented in Supporting information (Fig. S1 in Supporting information). The size, especially the depth of the nanochannel plays an important role in processing EVs, the fabrication procedure to control the size of the nanochannels are also described in the Supporting Information. When EVs pass through the nanochannels, mechanical compression and fluid shear lead to controlled mechanical deformation of EVs and increase their membrane permeability, therefore improving and accelerating the conjugation of fluorescent dyes on the phospholipid bilayer.

To assess the purity of the isolated EVs from cell culture medium, western blotting (WB), nanoparticle tracking analysis (NTA) and transmission electron microscopy (TEM) are performed, respectively. WB results show that the positive markers of EVs, *i.e.*, CD81 and TSG101, are enriched in the isolated EV samples, and the negative marker Calnexin is expressed in H1299 cells but not in EV samples (Fig. 2d). NTA results show that size of the isolated EVs ranges from 50 nm to 300 nm, and about 75% from 100 nm to 200 nm (Fig. 2e). EV sample treated by the labelling platform has no obvious change in size when compared with incubation (Fig. 2f). In addition, TEM is performed to observe morphology of the EVs with different treatments (Figs. 2g-i), a clear membrane structure with round-like and cap-shaped morphology is well maintained, and the EVs' lipophilic membrane keeps intact after the mechanical stimulation.

Before the EV labelling efficiency detection, FCM instrument is calibrated by a set of nanoparticle beads (Fig. S2 in Supporting information). Optimization on the experimental procedure is shown in Fig. S3 (Supporting information). The effect of nanochannel depth and flow rate on the labelling efficiency is presented in Fig. S4 (Supporting information). In order to validate the function of the microfluidic platform, fluorescent dye PKH67 is used, and the optimization on the dye concentration is described in Fig. S5 (Supporting information). The experimental schematics are shown in Fig. 3a. According to FCM results on fluorescent particle analysis, the labelled EVs in full-size range reach 16.37% and 26.29% for the Incubation group and the Chip group, respectively, the Chip group has a relative improvement of 60.59% on the labelling efficiency compared to the Incubation group (Fig. 3b). Moreover, according to the NTA results, more than 75% of EVs are of sizes between 100 nm and 200 nm. Thus, the EV labelling efficiency in different size ranges is analysed. As shown in Fig. 3c, more significant improvements in labelling efficiency are observed at EVs of 100 nm to 200 nm in the Chip group, where the labelled EVs in the 100 nm to 200 nm size range is 16.96% and 27.83% for the Incubation group and the Chip group (Figs. 3d-f), respectively, demonstrating that the Chip group has a relative improvement of 64.10% on the labelling efficiency compared to the Incubation group. The working mechanism for the improvement of labelling includes two aspects: (1) At the nanochannels, mechanical compression and fluid shear assist EV membrane permeabilization and relaxation without impacting EV morphology, therefore increasing the binding efficiency of EV membrane and lipophilic dye [27,28]. However, this phenomenon will disappear after EVs pass through the nanochannels and are collected at the outlet. (2) EVs and fluorescent dyes go through the inlet microchannels, nanochannels, and outlet microchannels subsequently. The rapid change of liquid flow characteristics may bring disturbance between two materials and increase the chance of collision [22,23]. Moreover, the dye aggregation of the Chip group is significantly decreased compared to the Incubation group (Fig. S6 in Supporting information).

Accurate EV labelling techniques are extremely important for subsequent experiments, such as cellular uptake, biodistribution *in vivo*. However, due to the influence of EV size and physicochemical properties of fluorescent dyes, false fluorescent signals are always generated, disturbing the accuracy of conclusions. In this work, our microfluidic platform can increase the labelling efficiency of EVs and decrease the detection background noise by using extremely low fluorescent dye concentration, which will improve EV detection accuracy in the FCM experiments and be beneficial for the follow-up EVs quantification and analysis.

Inspired by the above observations, we subsequently perform a cellular uptake experiment to assess spatial and temporal distribution of the labelled EVs in cells and to observe expression difference of intracellular EVs' fluorescence intensity. Fig. 4 shows fluorescence images of the uptake assay for a 12-h period. There is almost no PKH67 labelled-EVs' fluorescence appeared at 1 h in the view (green fluorescence) (Fig. 4a). A few EVs appeared at the perinuclear region after 4 h, and the fluorescent intensity of the Chip

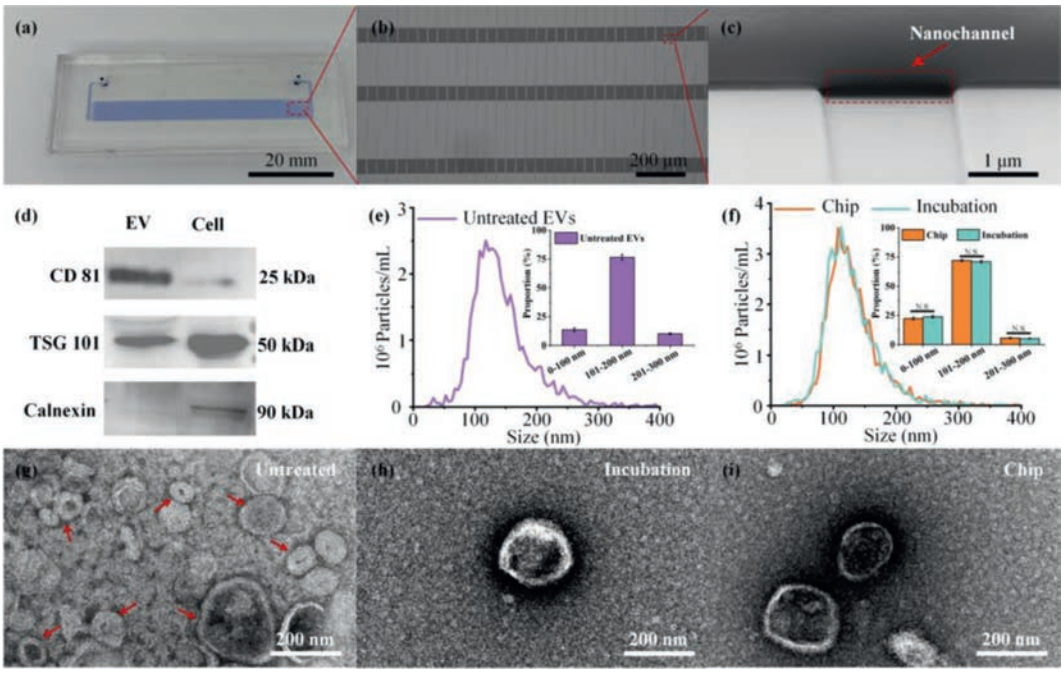

Fig. 2. Characterization of the microfluidic platform and EVs. (a) Photograph of the microfluidic platform. (b) Microscopic image on the parallel nanochannels bridging adjacent microchannels. (c) SEM image of the nanochannel in the microfluidic platform. (d) WB on EV positive protein markers (CD81, TSG101) and negative protein marker (Calnexin). (e) NTA characterization of the untreated EVs. (f) NTA characterization of the labelled-EVs treated by Chip and Incubation. TEM results of the EVs obtained from (g) untreated, (h) conventional incubation (Incubation) and (i) microfluidic platform treated (Chip) groups, respectively.

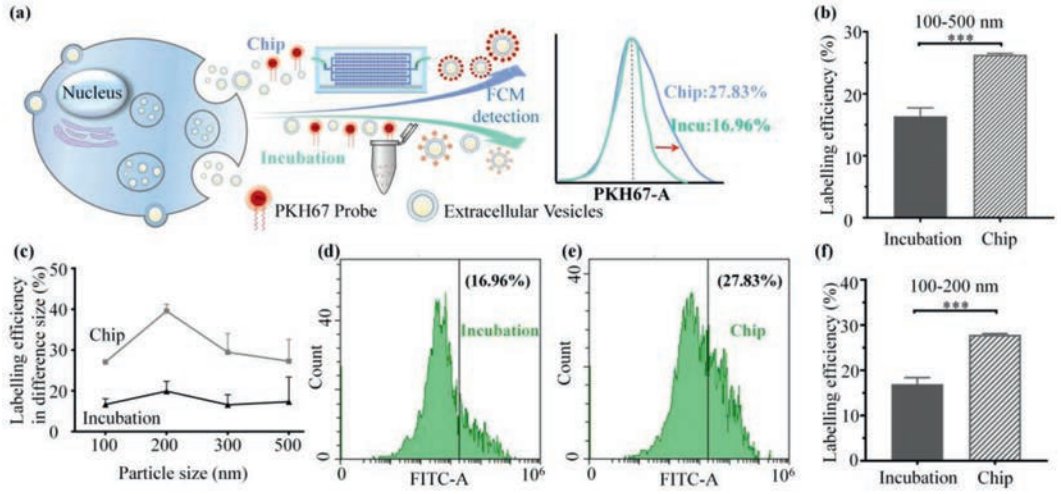

Fig. 3. Validation on the microfluidic platform function for EV fluorescent labelling. (a) Schematic illustration of the EV labelled with PKH67 dye by two methods. (b) A comparison of EV labelling efficiency between the Incubation group and the Chip group in full-size range. (c) EV labelling efficiency in different size ranges. A comparison of EV labelling efficiency between Incubation (d) and Chip (e) treatment in 100 nm to 200 nm size range, (f) is obtained from (d) and (e). *** $P < 0.001$.

group is higher than that of the Incubation group (Fig. 4b). After 12 h, a few green fluorescence spots are co-located with the blue fluorescence region, this means that EVs may enter the H1299 cells nuclear (Fig. 4c). From the co-localization analysis, appear around the nucleus after 4 h, and finally, after 12 h, almost all EVs enter the nucleus and involve in various life activities of the cells (*i.e.*, the cell migration). During the cellular uptake experiment, the amount of PKH67-labelled EVs is obviously increased in the view, the highest uptake, as assessed by fluorescence intensity, is observed from the Chip group after 12 h, with a notable difference compared to the Incubation group. It is worth noting that due to the low concentration of dyes used in this experiment, the fluorescence intensity is extremely weak in all dye control groups (Fig. S7 in Supporting information). Taken together, these results demonstrate our designed microfluidic labelling technology on EVs without excessive false positive signals, and the labelling efficiency is better than incubation, meeting the experimental requirements for FCM detection.

To investigate the biological activity of the EVs treated by the microfluidic platform, cell migration and CCK-8 assays are performed. The CCK-8 result is shown in Fig. S8 (Supporting information). The cell migration results are shown in Fig. 5, the EV group (both EV Chip and EV Control) presents an obvious trend of promoting cell migration in comparison to medium culture alone (Figs. 5a-f), the wound areas are presented in Fig. 5g. The cell migration area of H1299 cells after cultured with labelled EVs is 0.51 mm^2 and 0.49 mm^2 for the EV Control and EV Chip, respectively, without significant difference (Fig. 5h). According to previous stud-

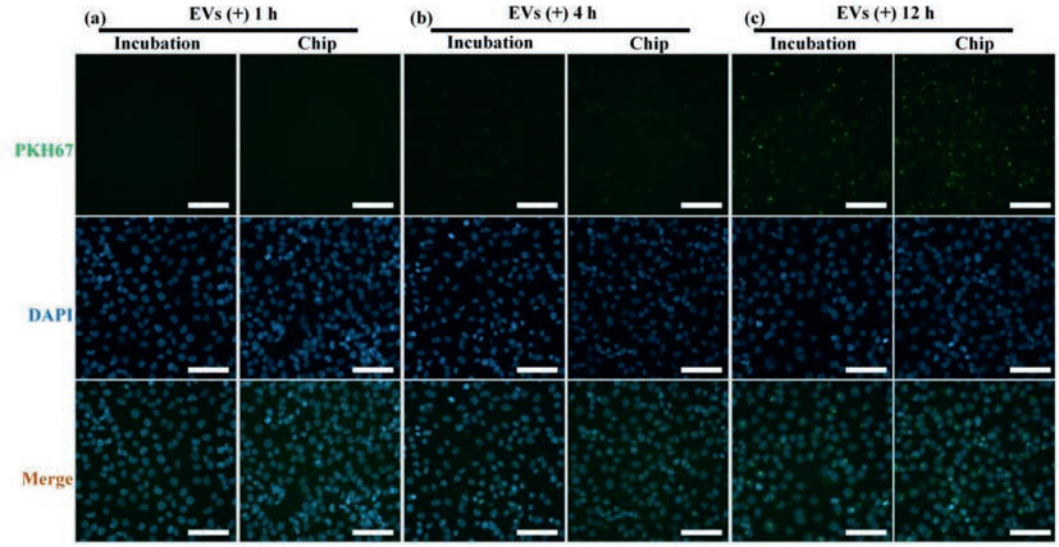

Fig. 4. Fluorescence microscopic images of H1299 cells incubated with EVs. PKH67-labelled EVs (green), DAPI (blue) and merge at (a) 1 h, (b) 4 h, and (c) 12 h after EVs (platform-treated and conventional incubated) are added into the well, respectively (Scale bars: 100 μm).

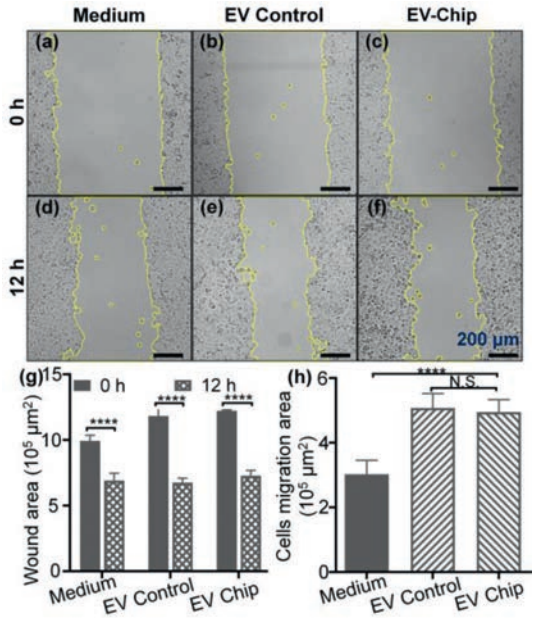

Fig. 5. Migration and viability tests of H1299 cells treated by culture medium and dye-labelled EVs. (a-f) Microscopic images of cell migration at 0 and 12 h. (g) Scratching area obtained from (a-f). (h) H1299 cells migration area with different treatments after 12 h (**** $P < 0.0001$).

ies, EVs secreted by tumour cells can promote cytoskeletal remodelling through fibronectin, the formation of aggressive pseudopodia, *i.e.*, increasing cell migration to promote tumour metastasis [29–31]. This phenomenon is in accordance with the results of the cell migration assay, indicating that our designed microfluidic platform has no negative impact on the biological activities of EVs.

In summary, we have designed a microfluidic platform that addresses the question of how to reduce false fluorescence signals generated by dye aggregation when quantifying sub-micron EVs. By resetting the EVs' phospholipid bilayer arrangement and increasing the probability of fluorescent dye incorporating with the EV membrane at extremely low dye concentrations, we hereby provide a new solution. Our platform has a higher labelling efficiency with a relative improvement of 64.10% on EVs of 100 nm to 200 nm in size when compared to conventional co-incubation labelling method. We think that in future, due to the straightforwardness of this approach, the proposed EV labelling technique by utilizing the microfluidic platform will develop into a robust and versatile technique that can be used to increase the labelling efficiency whilst reducing false positive signals, and eventually benefit precise quantification and measurement of EVs.

Declaration of competing interest

The authors declare that they have no known competing financial interest or personal relationship that could have appeared to influence the work reported in this paper.

Acknowledgments

This work is supported by the National Natural Science Foundation of China (Nos. 62074155, 62204253 and 62205366), Guangdong Program (No. 2016ZT06D631), Guangdong Basic and Applied Basic Research Foundation (Nos. 2020A1515110938 and 2020A1515110142), Shenzhen Science and Technology Innovation Committee (Nos. KCXFZ202002011008124 and JCYJ20210324101405016). We also thank Dr. Ke Liu (Resuntech Co., Ltd., Shenzhen) for the resistive pulse sensing analysis of EVs on Nanocoulter counter.

Supplementary materials

Supplementary material associated with this article can be found, in the online version, at doi:10.1016/j.cclet.2023.108534.

References

[1] R. Kalluri, V.S. LeBleu, Science 367 (2020) eaau6977.
[2] F.J. Verweij, L. Balaj, C.M. Boulanger, et al., Nat. Methods 18 (2021) 1013–1026.
[3] L.A. Mulcahy, R.C. Pink, D.R.F. Carter, J. Extracell. Vesicles 3 (2014) 24641.
[4] A. Latifkar, Y.H. Hur, J.C. Sanchez, et al., J. Cell Sci. 132 (2019) jcs222406.
[5] D.A. Borrelli, K. Yankson, N. Shukla, et al., J. Control. Release. 273 (2018) 86–98.
[6] E. Eren, J.F.V. Hunt, M. Shardell, et al., Alzheimer's Dement. 16 (2020) 1293–1304.
[7] J.L. Welton, S. Loveless, T. Stone, et al., J. Extracell. Vesicles 6 (2017) 1369805.
[8] D. Fortunato, D. Mladenović, M. Criscuoli, et al., Int. J. Mol. Sci. 22 (2021) 10510.
[9] E. Lázaro-Ibáñez, F.N. Faruqu, A.F. Saleh, et al., ACS Nano 15 (2021) 3212–3227.
[10] K.O. Jung, Y.H. Kim, S.J. Chung, et al., Int. J. Mol. Sci. 21 (2020) 7850.

[11] P. Lara, S. Palma-Florez, E. Salas-Huenuleo, et al., J. Nanobiotechnol. 18 (2020) 20.
[12] T. Vagner, A. Chin, J. Mariscal, et al., Proteomics 19 (2019) 1800167.
[13] S. Gandham, X. Su, J. Wood, et al., Trends Biotechnol. 38 (2020) 1066–1098.
[14] A. Mondal, K.A. Ashiq, P. Phulpagar, et al., Biol. Proced. Online 21 (2019) 4.
[15] A.E. Russell, A. Sneider, K.W. Witwer, et al., J. Extracell. Vesicles 8 (2019) 1684862.
[16] K. Takov, D.M. Yellon, S.M. Davidson, J. Extracell. Vesicles 6 (2017) 1388731.
[17] Y.J. Li, J.Y. Wu, J.M. Wang, et al., J. Control. Release 328 (2020) 141–159.
[18] T. Shimomura, R. Seino, K. Umezaki, et al., Bioconjugate Chem. 32 (2021) 680–684.
[19] H. Yang, M.A.M. Gijs, Chem. Soc. Rev. 47 (2018) 1391–1458.
[20] A. Kollmannsperger, A. Sharei, A. Raulf, et al., Nat. Commun. 7 (2016) 10372.
[21] F. Zhu, Y. Ji, J. Deng, et al., Chin. Chem. Lett. 33 (2022) 2893–2900.
[22] H. Kim, K.I. Min, K. Inoue, et al., Science 352 (2016) 691–694.
[23] H.J. Lee, Y. Yonekura, N. Kim, et al., Org. Lett. 23 (2021) 2904–2910.
[24] Y. Mo, Z. Lu, G. Rughoobur, et al., Science 368 (2020) 1352–1357.
[25] J. Ren, M. Wu, K. Dong, et al., Chin. Chem. Lett. 34 (2023) 107694.
[26] M. Mineo, S.H. Garfield, S. Taverna, et al., Angiogenesis 15 (2012) 33–45.
[27] A. Liu, M. Islam, N. Stone, et al., Mater. Today 21 (2018) 703–712.
[28] R. Hao, Z. Yu, J. Du, et al., Small 17 (2021) 2102150.
[29] N. Seo, K. Akiyoshi, H. Shiku, Cancer Sci. 109 (2018) 2998–3004.
[30] E.R. Matarredona, A.M. Pastor, Cells 9 (2020) 96.
[31] L. Chen, Z. Feng, H. Yue, et al., Nat. Commun. 9 (2018) 4585.